Control of Laminar Separation Bubbles by Small-Amplitude 2D and 3D Boundary-Layer Disturbances

Kai Augustin, Ulrich Rist, Siegfried Wagner
Universität Stuttgart
Institut für Aerodynamik und Gasdynamik
Pfaffenwaldring 21, 70550 Stuttgart, Germany

rist@iag.uni-stuttgart.de

ABSTRACT

Laminar separation bubbles in a flat-plate boundary layer flow with a velocity drop of 10%, 20%, and 25% applied locally at the free-stream boundary of the integration domain have been investigated by means of direct numerical simulations. Different steady and unsteady boundary layer disturbances were introduced at a disturbance strip upstream of separation and their effects on the separation bubble have been studied in 2-d and 3-d simulations. Generally, the same phenomena appear in both cases, i.e. the size of the separated region can be controlled by initially small 2-d disturbances, which grow to large levels by the hydrodynamic instability of the flow. Such unsteady disturbances, have a stronger impact on the size of the bubble than steady disturbances. Without loosing much efficiency, the pure 2-d forcing can be replaced by a three-dimensional forcing that produces obliquely travelling waves. The decisive parameter to influence the size of the separation bubble is the location of non-linear saturation of the disturbance modes, which may, but doesn't necessarily coincide with the location of transition to full turbulence.

1.0 INTRODUCTION

A transitional laminar separation bubble (LSB) is characterized by laminar separation (S) because of an adverse pressure gradient, laminar-turbulent transition (T), and turbulent re-attachment (R). Despite the occurrence of negative skin friction within the bubble LSBs may cause an undesired drag rise because of a considerable influence on the global pressure distribution of the airfoil. Unfortunately, their spatial extent is difficult to predict by theory or in wind-tunnel experiments, because of their Reynolds-number dependence and their sensitivity to background disturbances which are difficult to take into account. Small environmental changes may have a sudden influence and operating an airfoil at "off-design conditions" can make it prone to LSBs. However, such considerations will become completely obsolete once a suitable separation-bubble control becomes available for operational use. The key of LSB control is to control laminar-turbulent transition since an earlier transition will move the re-attachment upstream.

Existing systems to avoid the formation of LSBs involve the generation of turbulence upstream of the separation. Most often used turbulators apply zigzag or dimple tape mounted on the surface of the airfoil. Other devices use vortex generators [6] or constant blowing of air through holes in the surface of the airfoil [5] to generate-large scale streamwise vortices. For such active blowing devices a complicated system to provide the necessary bleed air might be necessary. All these systems have in common that they have to be developed for an optimum design point. Therefore, these systems cannot capture off-design conditions like different speed tasks of sail planes optimized for thermal flights. Active-blowing devices can be switched off at off-design conditions, but nevertheless additional disturbances may be generated by secondary flow through the holes in the presence of pressure gradients in the spanwise direction of the airfoil. Active systems which deform the surface of the airfoil to introduce disturbances into the flow

represent a solution to these problems. Switched off, these systems would no longer be a source of additional drag. As a drawback these systems only provide very small deformation amplitudes and imply electric driving and control devices. Moreover, a complex integrated sensor, controller and actuator system becomes desirable to become independent of any external interference with the system by the pilot. As maximum efficiency is the aim, according active turbulators have to be low-energy consuming and thin layered to fit into the limited space available on an airfoil besides the required supporting structural components. Nevertheless, such surface-mounted active devices can generate high-frequency perturbations which are necessary to introduce Tollmien-Schlichting-type boundary-layer disturbances into the flow. Due to hydrodynamic instability of the LSB flow, these boundary-layer disturbances become strongly amplified which leads to laminar-turbulent transition despite of their low initial disturbance amplitude. By introducing boundary-layer perturbations at a disturbance strip upstream of the separation into the laminar flow, transition can be triggered and therefore the size of the LSB be influenced. In the present work LSB flows are investigated in detail by means of linear stability theory [12] and direct numerical simulations (DNS) to evaluate methods using disturbance modes with different excitation parameters with respect to their impact on the size of typical mid-chord LSBs under different adverse pressure gradients.

2.0 NUMERICAL METHOD

To study laminar separation bubbles multiple direct numerical simulations (DNS) of a flat-plate boundary layer have been performed. An adverse pressure gradient is applied locally at a given distance from the inflow at the free-stream boundary to force separation. The code used for the present DNS has been used in different research programs for the investigation of transitional boundary layers with or without separation, cf. [7][8][11][14][16][17].

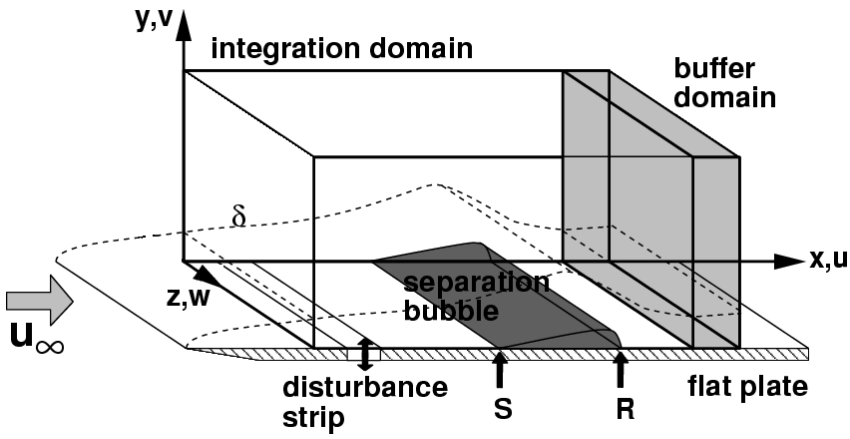

Figure 1: Integration domain

Figure 1 displays a sketch of the rectangular integration domain together with a definition of the coordinates and the respective velocity components. All variables are non-dimensionalized with respect to the free-stream velocity U_∞ and a reference length L which leads to a reference Reynolds number $Re = 100000$. The complete Navier-Stokes equations for incompressible flows are solved in a vorticity-velocity formulation [16]. A fourth-order accurate numerical method is applied in time and space by finite differences in streamwise and wall-normal direction and by a four step explicit Runge-Kutta scheme in time. For the spanwise direction a spectral ansatz implying periodic boundary conditions in that direction is used. Due to this the Poisson equations for the streamwise and spanwise velocity reduce to ordinary differential equations. The remaining 2-d Poisson equation for the wall-normal velocity is solved by a line

relaxation method accelerated by a non-linear multi-grid algorithm, once the vorticity-transport equations have been advanced to the next Runge-Kutta step. All equations can be solved separately for each spanwise spectral mode k allowing effective parallelization.

At the inflow boundary a Blasius boundary layer solution with a momentum thickness Reynolds number $Re^* = U_\infty \cdot \delta^* / \upsilon = 1722$ is prescribed. At the surface of the plate the no-slip boundary condition is applied except for a disturbance strip upstream of the LSB where periodic 2-d and 3-d boundary layer disturbances are introduced into the flow by suction and blowing. The streamwise length of the disturbance strip has been set to one wavelength of the most amplified disturbance mode according to linear stability theory (LST) and the beginning is located approximately two wavelengths downstream of the inflow boundary. For the total streamwise length of the integration domain *18.41* wavelengths have been used, and the height of the domain corresponds to *16* boundary-layer displacement thicknesses at the inflow. To avoid non-physical reflections at the outflow boundary the disturbance amplitudes are artificially damped in a buffer domain by several orders of magnitude, using the method described in [8].

The laminar separation bubble is induced by a local deceleration of the 'potential' free-stream velocity imposed via the u-component at the upper boundary as in [13]. Because of Bernoulli's equation this corresponds to imposing an adverse pressure gradient. The displacement effects of the LSB on the potential flow are captured by a viscous-inviscid boundary layer interaction model at every time step of the calculation (cf. [11] and [10]). Thus, the characteristic "pressure plateau" in the u-velocity distribution with a constant velocity in the upstream part of the separation bubble and a sharp velocity drop in the region of transition and re-attachment develops during the calculation (see next section).

3.0 NUMERICAL RESULTS

Three different streamwise velocity drops have been used for the following investigations: one with *10%*, one with *20%*, and one with *25%* reduction of free-stream velocity, where *10%* means a reduction from $U/U_\infty = 1$ to $U/U_\infty = 0.9$, for instance. In the following, these will be denoted *"case A"*, *"case B"*, and *"case C"*, respectively. A comparison of the three is performed in Figure 2 in terms of the "potential velocity" U_P, the resulting velocity U_M at the free-stream boundary, and in terms of the separation streamline $\Psi = 0$. Clearly, a larger velocity drop leads to a larger adverse pressure gradient and hence earlier separation at the wall. Also, the height of the bubble increases with rising pressure gradient. In all cases the typical "pressure plateau" develops in the velocity U_M (thick lines) as a result of the implemented viscous-inviscid interaction, as already anticipated above.

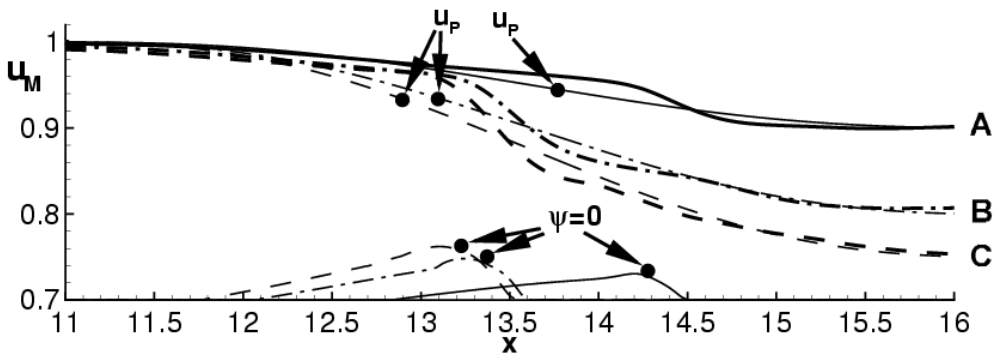

Figure 2: Comparison of prescribed potential flow (thin lines) with resulting free-stream velocity (thick lines) and separation streamlines for the three base flows with 10% (A, ———), 20% (B, – · – · –) and 25% velocity drop (C, – – –)

The following sections are intended to demonstrate how the laminar separation bubble in these base flows react on different means of unsteady upstream forcing. The basic idea is to control laminar-turbulent transition by introducing small-amplitude disturbance waves upstream of the LSB. If these are in the unstable frequency range they grow to large amplitudes. The earlier they reach a certain level, the earlier laminar-turbulent transition and the earlier turbulent re-attachment of the flow that closes the bubble.

Two-dimensional simulations are presented first because earlier simulations have shown that two-dimensional disturbances are most effective to control the laminar separation bubble [2][3] and because according 2-d simulations are much cheaper than 3-d ones. The second section will then show that this also holds in the present case, once the restriction to two dimensions is released. Towards the end the effects of using 3-d disturbances will be shown as well.

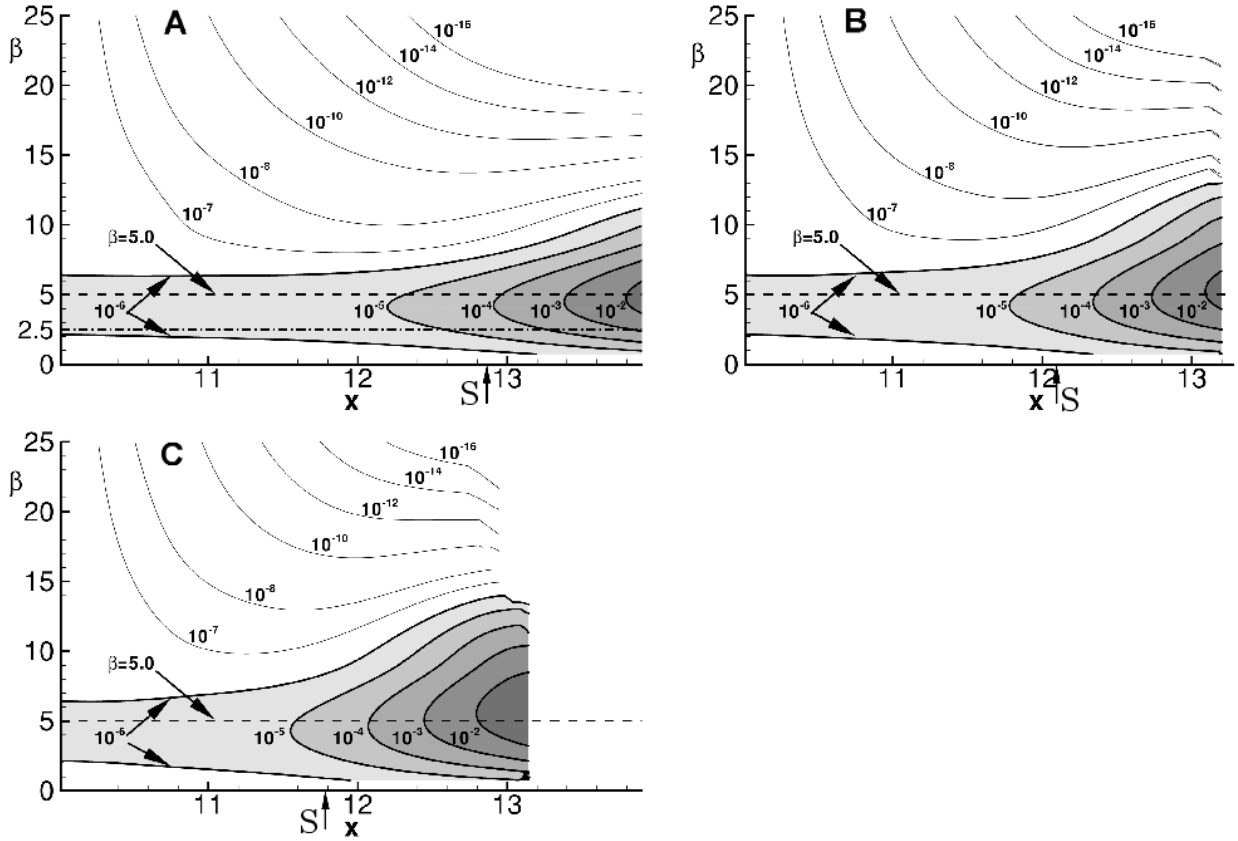

Figure 3: Disturbance amplification according to linear stability theory for the three base flows with 10% (upper left), 20% (upper right) and 25% velocity decrease (lower left); S = point of laminar separation

3.1 Effect of 2-d disturbances

Primary parameters for the specification of 2-d disturbances at the upstream disturbance strip are the wall-normal suction and blowing amplitude v' and the forcing frequency $\beta = 2\pi fL/U$, where f is the frequency in Hertz. An excellent overview about the possible range of useful disturbance frequencies is obtained from linear stability theory (LST). According results for all three base flows are shown in Figure 3 in terms of "amplification curves", i.e. integrated growth rates $A/A_0 = exp \int -\alpha_i \, dx$, starting with $A_0 = 10^{-6}$. Increasing amplitudes are indicated by increasing levels of gray. The figure points out that the instability of the flat-plate boundary layer develops seamlessly into that of a detached shear layer (downstream of

separation 'S'). Apparently, viscosity plays a role throughout the domain, despite the rather large Reynolds numbers in the present cases. The range of amplified frequencies is rather narrow and should be obeyed for an efficient bubble control strategy. For the following simulations the frequency $\beta = 5$ is chosen. It is indicated by the dashed line in the figure.

Here, the reader should remind that laminar-turbulent transition and its influence on the laminar separation bubble are both *non-linear* phenomena and that their prediction needs a full (non-linear) simulation, i.e. linear theory can only give a somewhat limited insight into the useful parameter range. It cannot predict laminar-turbulent transition and its impact on the bubble size. In addition, once the bubble has become smaller the linear instability of the flow is somewhat reduced. This effect is also contained in Figure 3, where the smallest bubble in "case A" exhibits lower amplification than the other two. The downstream distance that a disturbance must travel to grow, say from 10^{-6} to 10^{-2}, is accordingly largest in case A.

As just said, the investigation of the *non-linear* effects of unsteady forcing on the laminar separation bubble can so far only be investigated by full DNS. We therefore show results of one such simulation (frequency $\beta = 5$ and amplitude $v' = 10^{-6}$) in Figure 4 in terms of the time-averaged spanwise vorticity ϖ_z and the according instantaneous vorticity disturbance ω_z'. The steady laminar separation and the time-averaged re-attachment are indicated by arrows. The LSB is again designated by the separation streamline and the position of the disturbance strip by an according symbol at the wall. Downstream of the LSB a very high wall shear develops which resembles the high wall shear of a turbulent boundary layer despite the fact that only two-dimensional simulations have been performed and that a rather regular vortex shedding occurs in Figure 4 b). It turned out that the wall-normal momentum transfer induced by these vortices mimics the turbulent transport to a large extend. For instance, the shape parameter of the present boundary layer after re-attachment is close to $H = 2.0$ while the one for a turbulent boundary layer is $H = 1.4 - 1.5$. Inside the present bubble the shape factor rises to $H \approx 7$.

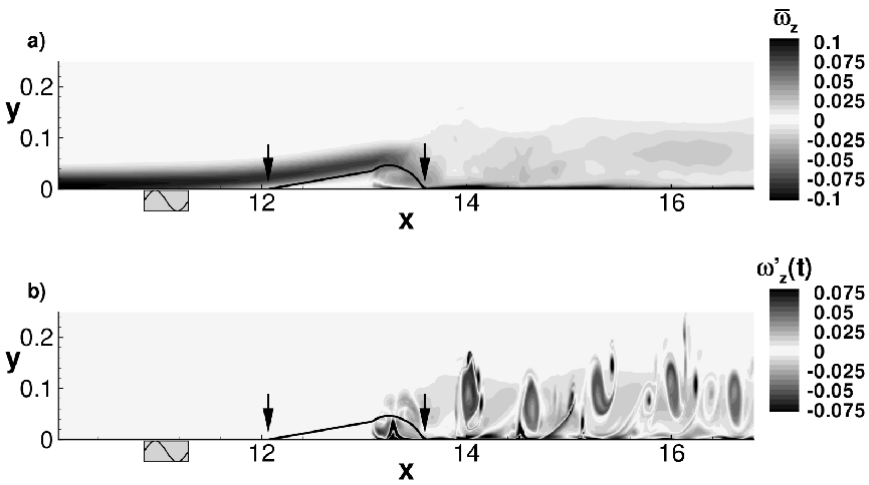

Figure 4: Comparison of time averaged vorticity (a) with instantaneous vorticity (b) for harmonic forcing of case B with 20% free-stream velocity drop

Upstream of $x \approx 13$ the disturbances are too small to be seen in a linear plot. We therefore use a representation in logarithmic scale in Figure 5. The lines depict the maxima of the wall-parallel velocity disturbance component u' for the fundamental mode *(1/0)* and its higher harmonic *(2/0)*, where *(h/k)* designates modes in the frequency (index h) spanwise wave number (index k) spectrum. The dash-dotted lines are results of LST along the line $\beta = 5$ in Figure 3. Both disturbances grow over several orders of magnitude until non-linear saturation which correlates with the formation of vortices in the previous figure. At vortex shedding the fundamental amplitude and its higher harmonic remain quasi constant.

Upstream of the disturbance strip the wave amplitudes decay to zero. The growth of the fundamental disturbance corresponds over a large extent to the one predicted by LST. The higher harmonic is generated as a product of the fundamental with itself and therefore amplifies faster than its according LST results (dash-dotted line with squares). The disturbances in base flow B with 20% velocity drop develop somewhat different. They exhibit an extremely sharp rise in amplitude just before saturation. Most probably this can be attributed to an absolute instability of the bubble due to some recirculation effects in its inside. In agreement with Figure 3, case C which has the highest velocity gradient and the largest separation bubble, shows the highest amplification and the most upstream position of non-linear saturation of disturbance mode *(1/0)* and therefore also its higher harmonic. Indications of an absolute instability are absent in this case.

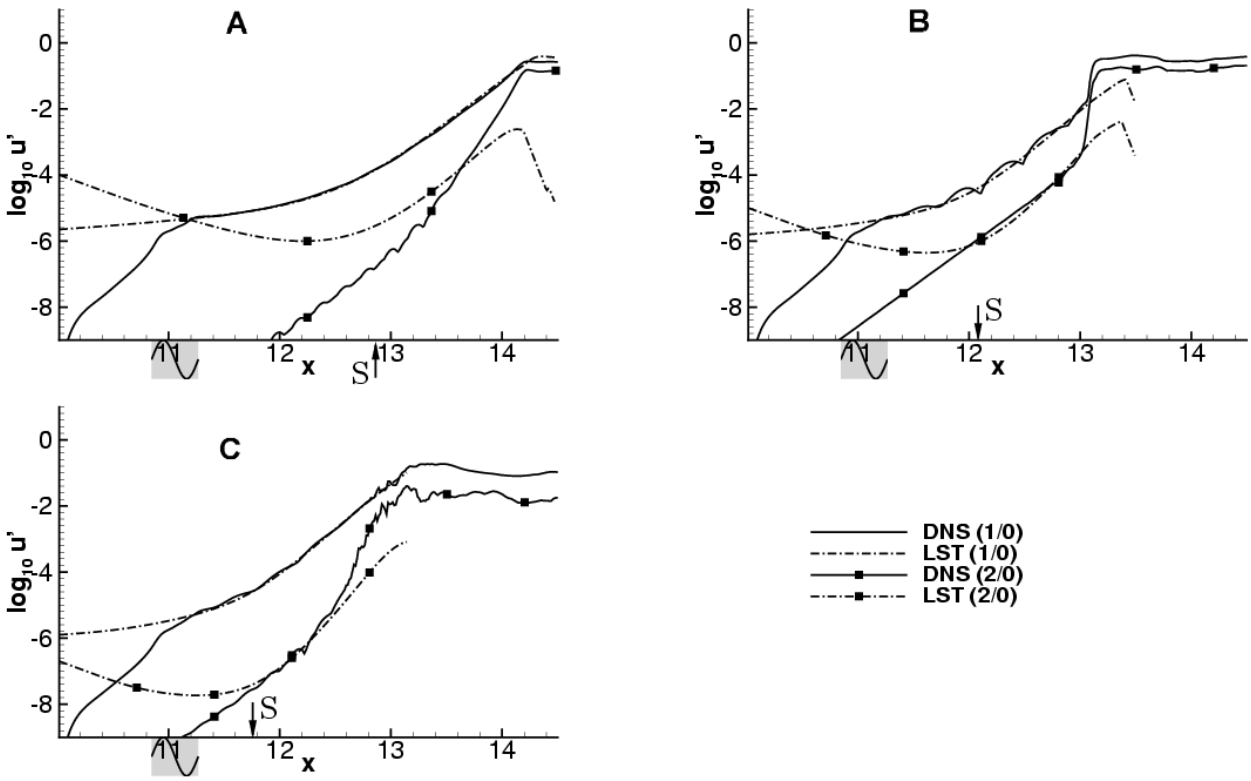

Figure 5: Amplification of fundamental disturbance *(1/0)* and its first harmonic *(2/0)* for the three different base flows, A: 10%, B: 20%, and C: 25% velocity drop; LST=linear stability theory

The effect of increasing disturbance amplitudes *v'* of the fundamental mode *(1/0)* are shown in Figure 6 for base flow B. The amplitude has been increased by a factor of *10* from one sub-figure to the next, i.e. by several orders of magnitude with respect to the first case. Again, the time-averaged separation streamline has been included and separation and mean re-attachment are indicated by arrows. In these 2-d simulations the size of the separation bubble has successfully been influenced until its almost removal. The vortices in the re-attachment region, which are responsible for the transport of momentum-rich fluid towards the wall to cause re-attachment, become smaller and more regularly spaced with higher forcing. In addition, the higher harmonic *(2/0)* has also grown to such a large level that it produces smaller vortices in-between the primary ones. Since the instability of the base flow decreases once the size of the LSB gets smaller, the additional energy input to influence the LSB increases in a non-linear manner. Initially this increase is exponential as can be seen from an evaluation of the separation- and re-attachment-point positions as well as the bubble length from case A in Figure 7.

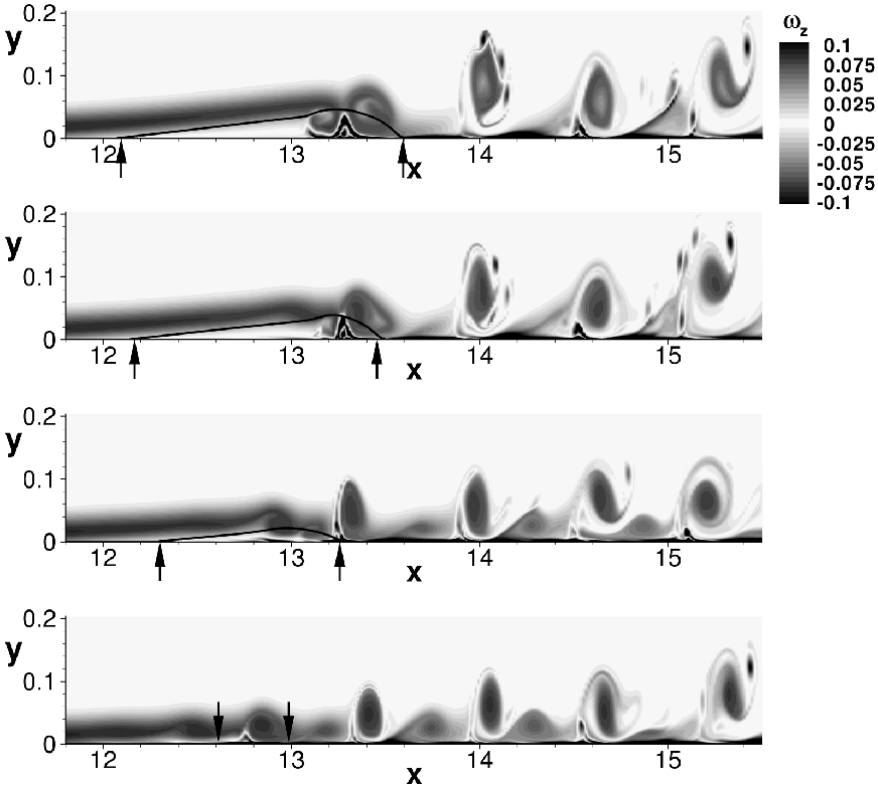

Figure 6: Instantaneous vorticity for increasing forcing amplitudes *v'* = 10^{-6}, 10^{-5}, 10^{-4}, and 10^{-3} (top to bottom) in base flow B

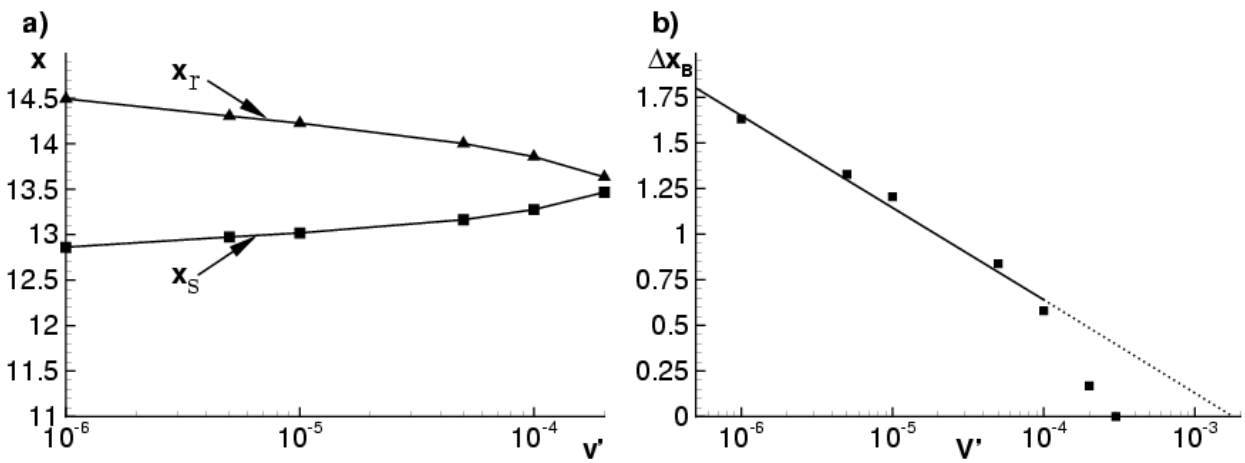

Figure 7: Evolution of separation position x_s and re-attachment position x_r with disturbance amplitude *v'* (a); evolution of bubble length (b); base flow A with *10%* velocity drop

3.2 Role of 3-d disturbances

Three-dimensionality may have two kinds of influence on the present problem. First, suppression of the third dimension in our previous simulations has for sure inhibited turbulence which is inherently three-dimensional. Therefore, the next subsection will show a comparison of a full 3-d simulation with a previous 2-d one. Second, three-dimensional disturbance input may also be used to control the present

laminar separation bubbles. In practice this might be easier to realize than a "perfect 2-d" forcing. Such questions will be investigated in subsection 3.2.2.

3.2.1 Influence of the third dimension

To add an additional degree of freedom in the simulations, cases A and B have been extended to 3-d. This, of course, introduces the spanwise wavenumber as an additional parameter. This was set to *5.4596* which corresponds to a spanwise wavelength of $\lambda_z = 0.8689$ and an angle of obliqueness of $\phi = 20^o$ referring to the 3-d fundamental disturbance *(1/1)*. Adding this disturbance is equivalent to adding a pair of oblique waves *(1/±1)* because of spanwise symmetry imposed by the spectral ansatz. In case A this didn't make any appreciable difference to the 2-d case. We therefore concentrate here on case B which showed traces of an absolute instability in the pure 2-d case in Figure 5. As already said, three-dimensionality was initialized with a 3-d mode *(1/1)* at $v' = 10^{-6}$ together with the 2-d mode *(1/0)*. Both disturbances grow according to LST and they are practically indistinguishable in Figure 8. Non-linearity then adds higher harmonic 3-d modes which grow in proportion to the spanwise wave number index *k*. In contrast to the 2-d case all modes now grow until non-linear saturation in close agreement with LST, i.e. the absolute instability from above doesn't appear any more. With respect to an according study of the boundary between convective and absolute instability in [10] and [18] it should be noted that the maximum reverse flow velocity amounts to *18.6 %* in the 2-d case and to *11.1 %* in the 3-d case, such that the present observations are in full agreement with these earlier observations. In addition to the arrows which point to the positions of laminar separation and re-attachment, laminar-turbulent transition is indicated by the letter 'T' and a vertical line placed at the maximum disturbance amplitude.

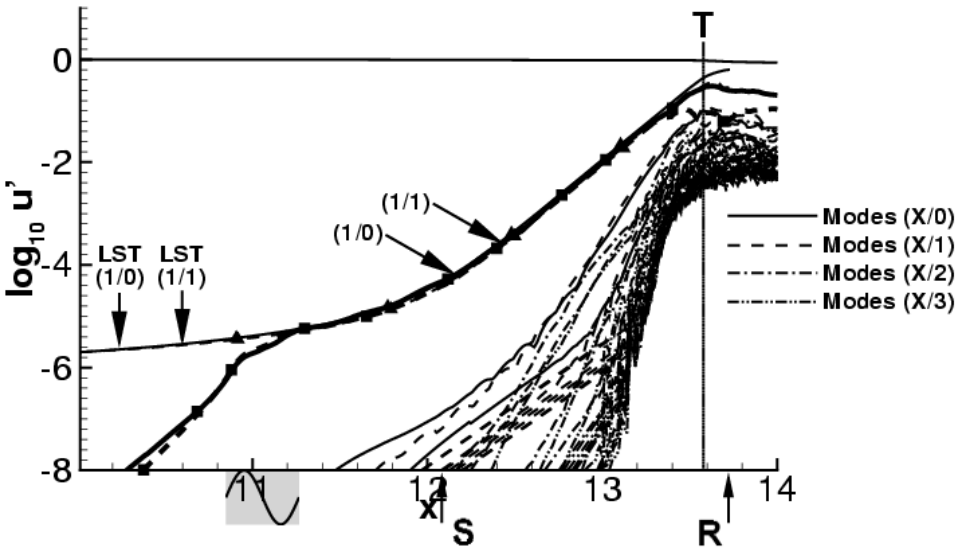

Figure 8: Two- and three-dimensional disturbance amplification in base flow B

This different disturbance behavior leads to differences in the mean-flow which are parameterized in Figure 9. The 3-d results are marked by squares. The shape parameter *H* is equal to the ratio of the displacement thickness with respect to the momentum thickness. $Re_{\delta 1}$ and $Re_{\delta 2}$ are the respective Reynolds numbers. In the 3-d case the bubble becomes longer and the shape parameter increases to larger values inside the bubble. Downstream of the bubble the 3-d shape parameter drops to much lower values than its 2-d counterpart which indicates that the boundary layer in the 3-d case resembles a turbulent boundary layer much closer (like in the case displayed in Figure 10). In addition, the corresponding curve is much smoother.

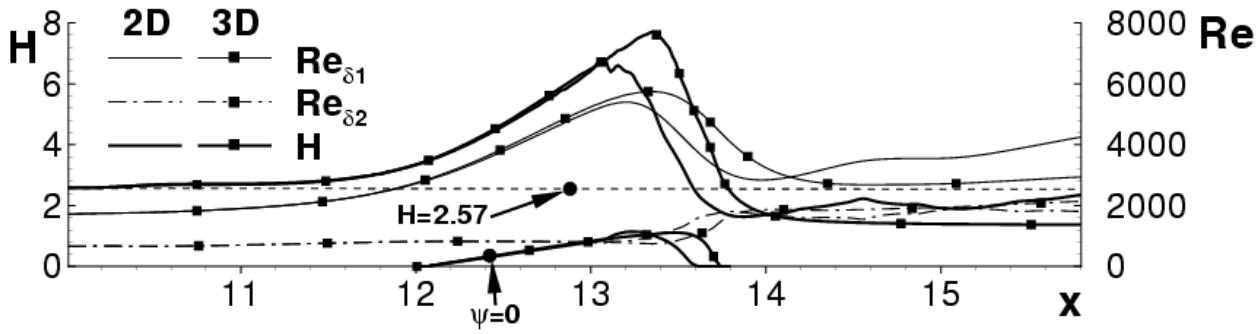

Figure 9: Comparison of boundary layer parameters of the 2-d simulations of base flow B with results of the 3-d simulations

A 3-d simulation with increased 2-d forcing (at $v' = 10^{-4}$) is considered next. This case can be compared to the pure 2-d simulation results shown above. A comparison of the instantaneous vorticity contours in Figure 10 with the third subfigure in Figure 6 nicely displays the breakdown of the boundary layer to small-scale 3-d structures after re-attachment. The bubble itself turns out to become somewhat smaller than above because of a delay of laminar separation. The flow inside the bubble and at re-attachment is still governed by large-amplitude 2-d vortex shedding. This is simply due to the increased 2-d forcing, i.e. a dominance of the 2-d mode *(1/0),* as can be seen in Figure 11.

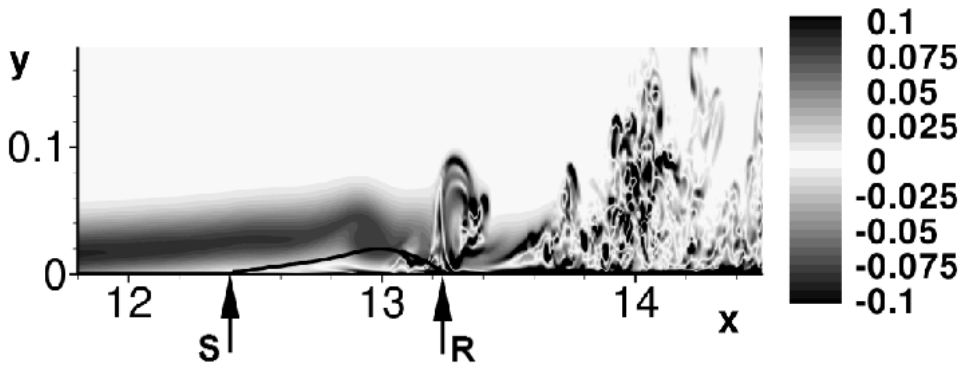

Figure 10: Instantaneous vorticity in the 3-d simulation of case B with increased 2-d forcing at $v'=10^{-4}$

Again, the primary modes *(1/0)* and *(1/1)* develop according to LST nearly until transition (T). However, the non-linear saturation starts smoother than before and it gets more difficult with increasing 2-d forcing amplitudes to define a reasonable position for laminar-turbulent transition. The spectrum after saturation is dominated by 2-d modes *(h/0)* while the 3-d modes saturate at one tenth of the maximum 2-d amplitude. After re-attachment the 2-d modes decrease, such that the 3-d breakdown of the previous figure becomes apparent for larger *x*.

The present comparisons of three- and two-dimensional simulations have shown that a 2-d control is very efficient because small disturbance amplitudes which can be generated using very little input energy are able to control the laminar-turbulent transition process and hence the laminar separation bubble. Adding the third dimension doesn't influence the efficiency, despite the fact that the laminar-turbulent breakdown process appears more realistic then. In most cases, the bubble is not critically affected by the third dimension. The worst case found has been shown above in Figure 9 because in that case three-dimensionality has changed the instability character of the bubble.

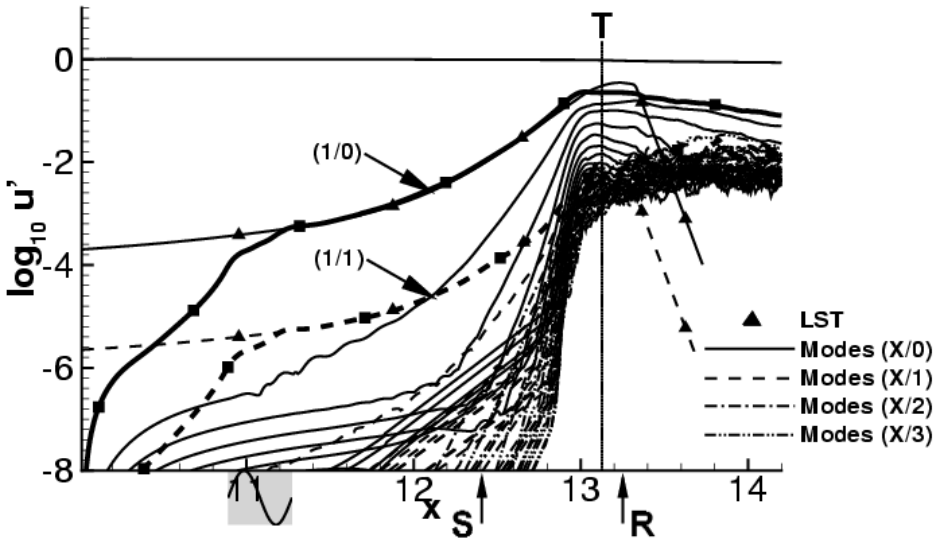

Figure 11: Disturbance amplification in base flow B with increased 2-d forcing at v'=10^{-4}

3.2.2 Effects of three-dimensional forcing

Because of the fact that 3-d disturbances can be generated much easier in practical applications than perfect 2-d ones, one has to consider the efficiency of using 3-d disturbances for laminar separation bubble control as well. This is done now based on the above base-flow case A (10% velocity drop at the free-stream boundary) and with a forcing amplitude $v' = 10^{-5}$ for the 3-d mode *(1/1)* (same spanwise wavenumber as before). The forcing of *(1/0)* is kept at its previous level of 10^{-6}. The disturbance amplification in Figure 12 indicates that mode *(1/1)* now dominates the whole process with the consequence that the 3-d higher harmonics grow to larger levels, i.e. 3-d turbulence sets in much earlier now. This has again some consequences on the separation bubble and its boundary layer parameters.

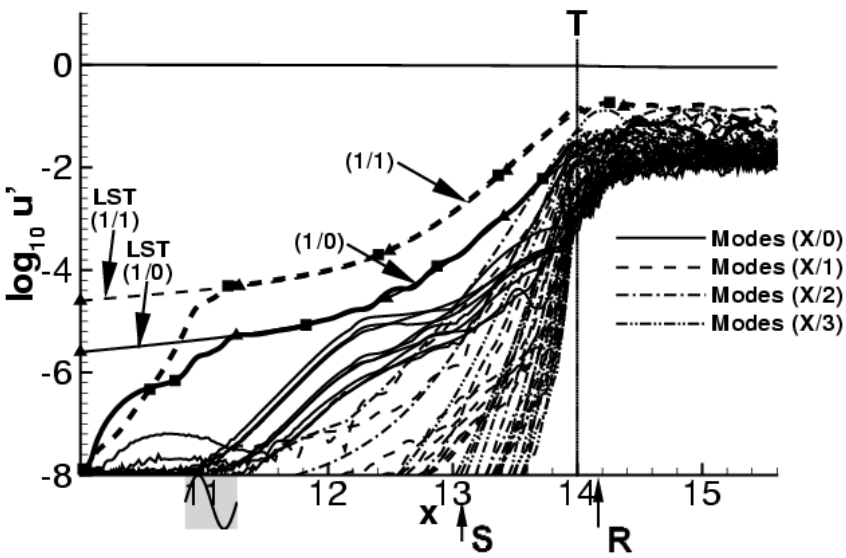

Figure 12: Disturbance amplification in base flow A with increased 3-d forcing at v'=10^{-5}

In Figure 13 the parameters of the case with increased 3-d forcing is identified with symbols. The reaction of the flow is comparable to a 10-fold increase of the 2-d amplitude: The length of the laminar separation

bubble decreases, and so does its height. Shape parameters and Reynolds numbers show an according difference. Because of a nearly identical growth of the 3-d disturbance *(1/1)* in comparison with the 2-d *(1/0)* the laminar separation bubble can be controlled by either of the two at practically the same efficiency. However, downstream of the bubble the full 3-d case delivers a flow that is closer to a turbulent one than in the other case, because of a lower shape parameter.

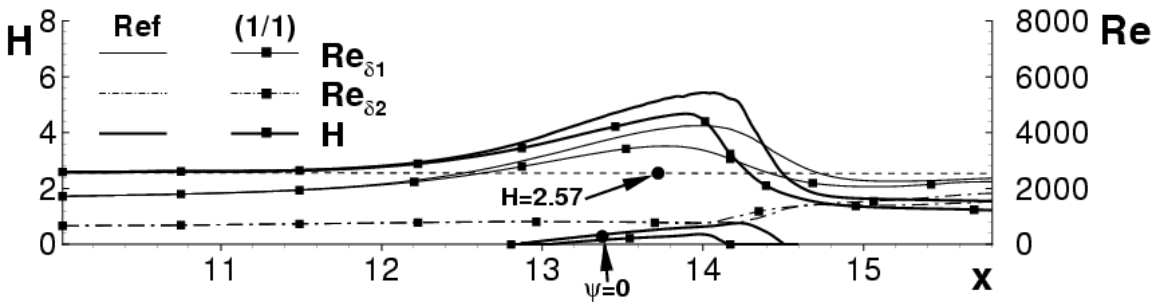

Figure 13: Comparison of boundary layer parameters of the 3-d simulations of base flow A with equal-amplitude 2- and 3-d forcing (Ref) and with increased 3-d forcing (1/1)

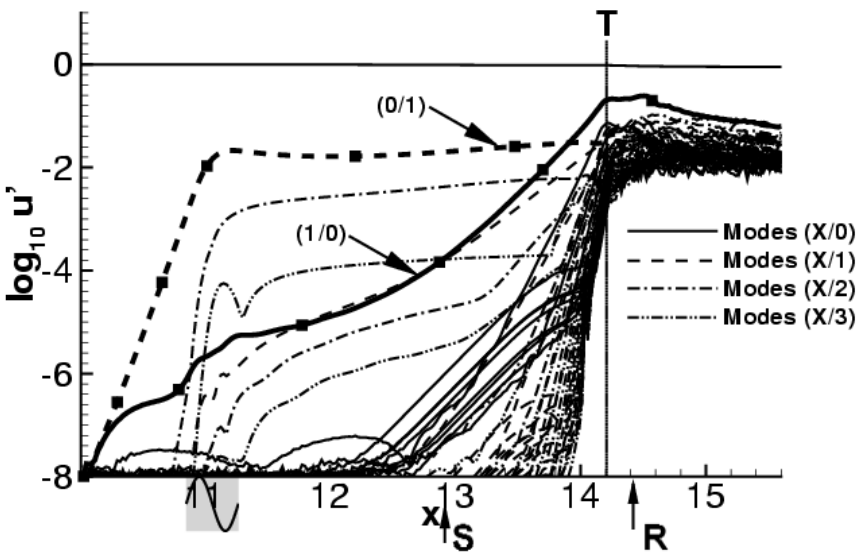

Figure 14: Disturbance amplification in base flow A subject to a steady 3-d disturbance (0/1)

Our next investigation will now show the effect of using a *steady* 3-d forcing to control the bubble. Such an approach is closer to "more traditional" techniques, like applying a row of small bumps upstream of separation to cause turbulence in order to prevent laminar separation. For this investigation the spanwise wavenumber has been increased to *15* which corresponds to a spanwise wave length of *0.4189* in the present scaling. To simulate such a steady 3-d 'roughness' mode *(0/1)* has been forced with $v' = 10^{-3}$ in addition to the other modes in the 3-d reference case for base flow A. The resulting disturbance growth of individual modes is shown in Figure 14. Initially, the spectrum is dominated by the steady 3-d mode and its higher harmonics, but in contrast to the traveling ones, they are only moderately amplified. More on the amplification of steady modes in a flow with LSB can be found in [9]. In the present case, this means that much larger initial amplitudes are needed with respect to the previous unsteady disturbances. Apparently, the laminar-turbulent transition process is not much affected by the additional steady disturbance, despite its large initial amplitude. This can be explained by the fact, that adding a steady

roughness doesn't directly produce turbulence (which is inherently unsteady). The latter can only occur when wall-roughness interacts with fluctuations of the free stream. Hence, in practice large roughness is needed to cause laminar-turbulent transition via some bypass-mechanism, i.e. one without linear amplification of disturbances (in contrast to the driving mechanism in the present investigations).

In accordance with the above discussion the boundary layer parameters in Figure 15 show that the effect of the steady 3-d forcing is decent, despite the *1000*-fold larger amplitude compared to the 2-d unsteady forcing above. The bubble shapes and the evolution of Reynolds numbers and shape factors remain practically unaltered.

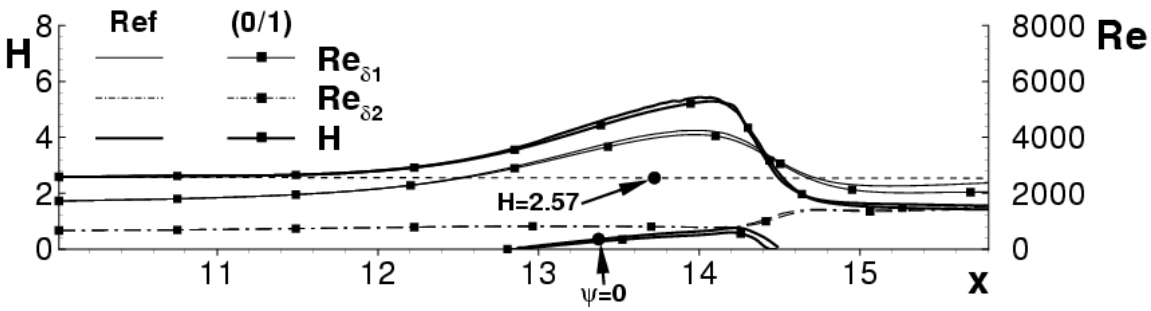

Figure 15: Comparison of boundary layer parameters of base flow A suspect to large-amplitude steady 3-d forcing (0/1) with the reference case (Ref)

A visualisation of the 3-d separation surface (i.e. an approximation of the surface that separates the time-averaged recirculating flow inside the bubble with the external stream) shows that the steady 3-d disturbance amplitude was indeed considerably large such that it causes longitudinal grooves in the bubble. Its inefficiency is hence not caused by a too-small amplitude.

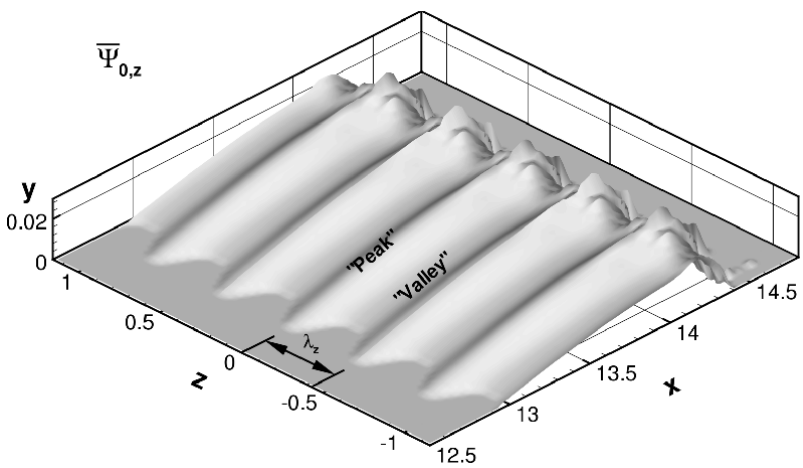

Figure 16: Separation stream surface of base flow A in case of large-amplitude steady 3-d forcing

4.0 CONCLUSIONS AND OUTLOOK

The above results show the advantages of the excitation of unsteady 2-d or 3-d disturbances rather than steady disturbances in separation control scenarios. In order to provide the necessary unsteady disturbance amplitude, a possible control system for LSBs would consist of a frequency generator, an amplifier and an

actuator, as already discussed in [4], mainly because it suffices to provoke laminar-turbulent transition by some appropriate means without an urgent need for some highly sophisticated controller. In fact, a simple switch that turns LSB control on or off when appropriate could be sufficient, once the different flow situations are understood well enough. As already shown in [4] the frequency generator could be replaced by a feed-back of instantaneous skin friction signals obtained from a position downstream of the separation bubble. The broad band of frequencies in the most unstable frequency range due to hydrodynamic instability then provides a robust signal source for the actuator, after an appropriate reduction to lower amplitudes. In a further step, distributed skin-friction sensors could be devised to detect the separation length via time-averaged skin-friction signals, which in turn could be used to control the feed-back amplitude gain, and hence the bubble.

REFERENCES

[1] Augustin, K. 2004/2005: Zur aktiven Beeinflussung von laminaren Ablöseblasen mittels Grenzschichtstörungen, Dissertation Universität Stuttgart.

[2] Augustin, K., Rist, U. & Wagner, S. 2001: Active control of a laminar separation bubble, Notes on Numerical Fluid Mechanics (NNFM) 76, Springer-Verlag, 297–303.

[3] Augustin, K., Rist, U. & Wagner, S. 2002: Active control of separation bubbles exploiting laminar base-flow instabilities, Proceedings of 2002 ASME-European FED Summer Annual Meeting. ASME, Montreal, Quebec, Canada.

[4] Augustin, K., Rist, U. & Wagner, S. 2003: Investigation of 2d and 3d boundary-layer disturbances for active control of laminar separation bubbles. 41st AIAA Aerospace Sciences Meeting and Exhibit, AIAA 2003–0613. Reno, NV, USA.

[5] Horstmann, K. H., Quast, A. & Boermans, L. M. M. 1984: Pneumatic turbulators – a device for drag reduction at Reynolds numbers below $5{\cdot}10^6$. AGARD CP-365, pp. 20-1–20-19.

[6] Kerho, M., Hutcherson, S., Blackwelder, R. F. & Liebeck, R. H. 1993: Vortex generators used to control laminar separation bubbles. Journal of Aircraft 30 (3), 315–319.

[7] Kloker, M. 1998: A robust high-resolution split-type compact FD scheme for spatial direct numerical simulations of boundary layer transition. Applied Scientific Research 59 (4), 353–377.

[8] Kloker, M., Konzelmann, U. & Fasel, H. 1993: Outflow boundary conditions for spatial Navier-Stokes numerical simulations of transition boundary layers. AIAA Journal 31 (4), 620–628.

[9] Marxen, O., Rist, U., Wagner, S. 2004: Effect of spanwise-modulated disturbances on transition in a separated boundary layer, AIAA Journal 42 (8), 937-944.

[10] Maucher, U. 2002: Numerische Untersuchungen zur Transition in der laminaren Ablöseblase einer Tragflügelgrenzschicht, Dissertation Universität Stuttgart.

[11] Maucher, U., Rist, U. & Wagner, S. 2000: Refined interaction method for direct numerical simulation of transition in separation bubbles. AIAA Journal 38 (8), 1385–1393.

[12] Reed, H., Saric, W. S. & Arnal, D. 1996: Linear stability theory applied to boundary layers. Ann. Rev. Fluid Mech. 28, 389–428.

[13] Rist, U. 1994: Nonlinear effects of two-dimensional and three-dimensional disturbances on laminar

separation bubbles. In Nonlinear Instability of Nonparallel Flows (ed. S. P. Lin). IUTAM Symposium, Potsdam, NY, USA: Springer Verlag.

[14] Rist, U. 1999: Zur Instabilität und Transition in laminaren Ablöseblasen. Habilitation, Universität Stuttgart, Shaker Verlag.

[15] Rist, U., Augustin, K. & Wagner, S. 2001: Numerical simulation of laminar separation bubble control. Notes on Numerical Fluid Mechanics (NNFM) 77, 170–177.

[16] Rist, U. & Fasel, H. 1995: Direct numerical simulation of controlled transition in a flat-plate boundary layer. J. Fluid Mech. 298, 211–248.

[17] Rist, U. & Maucher, U. 1994: Direct numerical simulations of 2-d and 3-d instability waves in a laminar separation bubble. In Application of Direct and Large Eddy Simulation of Transition and Turbulence, AGARD CP-551, pp. 34-1–34-7.

[18] Rist, U. & Maucher, U. 2002: Investigations of time-growing instabilities in laminar separation bubbles. European Journal of Mechanics B/Fluids 21, 495–509.

[19] Rist, U., Maucher, U. & Wagner, S. 1996: Direct numerical simulation of some fundamental problems related to transition in laminar separation bubbles. In Computational Methods in Applied Sciences ’96 , pp. 319–325. ECCOMAS, Paris, France: John Wiley & Sons Ltd.